Chiral Expression at the Solid−Liquid Interface: A Joint Experimental and Theoretical Study of the Self-Assembly of Chiral Porphyrins on Graphite

Mathieu Linares,[†] Patrizia Iavicoli,[‡] Krystallia Psychogyiopoulou,[§] David Beljonne,[†] Steven De Feyter,*[,§] David B. Amabilino,*[,‡] and Roberto Lazzaroni*[,†]

Service de Chimie des Matériaux Nouveaux, Université de Mons-Hainaut, 20, Place du Parc, B-7000 Mons, Belgium, Institut de Ciència de Materials de Barcelona (CSIC), Campus Universitari, 08193 Bellaterra, Catalonia, Spain, and Laboratory of Photochemistry and Spectroscopy, Molecular and Nano Materials, Department of Chemistry, and INPAC - Institute for Nanoscale Physics and Chemistry, Katholieke Universiteit Leuven, Celestijnenlaan 200-F, 3001 Leuven, Belgium

Received June 5, 2008

The chiral organization of an enantiopure functional molecule on an achiral surface has been studied with the aim of understanding the influence of stereogenic centers on the self-assembly in two dimensions. A chiral tetra *meso*-amidophenyl-substituted porphyrin containing long hydrophobic tails at the periphery of the conjugated π-electron system was prepared for this purpose. Scanning tunneling microscopy (STM) images of the compound at the graphite−heptanol interface reveal a chiral arrangement of the molecules, with the porphyrin rows tilted by 13° with respect to the normal to the graphite axes. In terms of molecular modeling, a combination of molecular dynamics simulations on systems constrained by periodic boundary conditions and on unconstrained large molecular aggregates has been applied to reach a quantitative interpretation on both the density of the layer and its orientation with respect to the graphite surface. The results show clearly that (i) the methyl groups of the stereogenic point toward the graphite surface and (ii) the porphyrin molecules self-assemble into an interdigitated structure where the alkyl chains align along one of the graphite axes and the porphyrin cores are slightly shifted with respect to one another. The direction of this shift, which defines the chirality of the monolayer, is set by the chirality of the stereogenic centers. Such an arrangement results in the formation of a dense chiral monolayer that is further stabilized by hydrogen bonding with protic solvents.

Introduction

Chirality has profound implications in physics,[1] chemistry,[2] materials science,[3] and biology.[4] Yet, the design of chiral arrangements with well-defined structures and properties is largely a hit-and-miss affair. To be able to take full advantage of the expression of chirality at the supramolecular scale, an in-depth analysis of the relationship between the various intermolecular interactions at play and the chiral character of the resulting assemblies is needed.

Chiral expression at surfaces has attracted significant attention only in recent years,[5] despite the fact that it is actually easier to create chirality in a 2D system than in 3D ones, since a surface cannot possess a center of inversion and can only maintain reflection mirror symmetry planes normal to the surface.[6] A wide variety of chiral systems have been generated by both physisorption[7] and chemisorption,[8] using either chiral or achiral molecules as the adsorbate.[5e,9] As a rule of thumb, chiral enantiopure molecules form enantiomorphous patterns. Just as enantiomers can be converted into each other by a mirror

* To whom correspondence should be addressed. E-mail amabilino@icmab.es (D.B.A.); steven.defeyter@chem.kuleuven.be (S.D.F.); Roberto@averell.umh.ac.be (R.L.).

[†] Université de Mons-Hainaut.

[‡] Campus Universitari.

[§] Katholieke Universiteit Leuven.

(1) (a) Ellis, J. *Nature* **2003**, *424*, 631. (b) Bode, M.; Heide, M.; von Bergmann, K.; Ferriani, P.; Heinze, S.; Bihlmayer, G.; Kubetzka, A.; Pietzsch, O.; Bluegel, S.; Wiesendanger, R. *Nature* **2007**, *447*, 190. (c) Kimura, T.; Otani, Y.; Masaki, H.; Ishida, T.; Antos, R.; Shibata, J. *Appl. Phys. Lett.* **2007**, *90*, 132501.

(2) (a) Attard, G. A. *J. Phys. Chem. B* **2001**, *105*, 3158. (b) Feringa, B. L.; van Delden, R. A. *Angew. Chem., Int. Ed.* **1999**, *38*, 3418. (c) Leigh, D. A.; Perez, E. M. *Top. Curr. Chem.* **2006**, *265*, 185.

(3) (a) Bradshaw, D.; Claridge, J. B.; Cussen, E. J.; Prior, T. J.; Rosseinsky, M. J. *Acc. Chem. Res.* **2005**, *38*, 273. (b) Zhang, J.; Albelda, M. T.; Liu, Y.; Canary, J. W. *Chirality* **2005**, *17*, 404. (c) Cancelliere, G.; D'Acquarica, I.; Gasparrini, F.; Maggini, M.; Misiti, D.; Villani, C. *J. Sep. Sci.* **2006**, *29*, 770. (d) Amabilino, D. B.; Veciana, J. *Top. Curr. Chem.* **2006**, *265*, 253. (e) Brettar, J.; Burgi, T.; Donnio, B.; Guillon, D.; Klappert, R.; Scharf, T.; Deschenaux, R. *Adv. Funct. Mater.* **2006**, *16*, 260.

(4) (a) Lough, W. J., Wainer, I. W., Eds. *Chirality in Natural and Applied Science*; CRC Press: Boca Raton, FL, 2002. (b) Carmeli, I.; Skakalova, V.; Naaman, R.; Vager, Z. *Angew. Chem., Int. Ed.* **2002**, *41*, 761. (c) Sun, T.; Han, D.; Rhemann, K.; Chi, L.; Fuchs, H. *J. Am. Chem. Soc.* **2007**, *129*, 1496.

(5) (a) Raval, R. *Curr. Opin. Solid State Mater. Sci.* **2003**, *7*, 67. (b) Nandi, N.; Vollhardt, D. *Chem. Rev.* **2003**, *103*, 4033. (c) Ernst, K.-H. *Top. Curr. Chem.* **2006**, *265*, 209. (d) Barlow, S. M.; Raval, R. *Surf. Sci. Rep.* **2003**, *50*, 201. (e) Plass, K. E.; Grzesiak, A. L.; Matzger, A. J. *Acc. Chem. Res.* **2007**, *40*, 287.

(6) (a) Weissbuch, I.; Kuzmenko, I.; Berfeld, M.; Leiserowitz, L.; Lahav, M. *J. Phys. Org. Chem.* **2000**, *13*, 426. (b) Weissbuch, I.; Leiserowitz, L.; Lahav, M. *Top. Curr. Chem.* **2005**, *259*, 123.

(7) (a) Samorí, P.; Yin, X.; Tchebotareva, N.; Wang, Z.; Pakula, T.; Jäckel, F.; Watson, M. D.; Venturini, A.; Müllen, K.; Rabe, J. *J. Am. Chem. Soc.* **2004**, *126*, 3567. (b) Lu, J.; Lei, S.-b.; Zeng, Q.-d.; Kang, S.-z.; Wang, C.; Wan, L.-j.; Bai, C.-l. *J. Phys. Chem. B* **2004**, *108*, 5161. (c) Abdel-Mottaleb, M. M. S.; Gomar-Nadal, E.; Surin, M.; Uji-I, H.; Mamdouh, W.; Veciana, J.; Lemaur, V.; Rovira, C.; Cornil, J.; Lazzaroni, R.; Amabilino, D. B.; De Feyter, S.; De Schryver, F. C. *J. Mater. Chem.* **2005**, *15*, 4601. (d) Sakurai, S.-i.; Okoshi, K.; Kumaki, J.; Yashima, E. *J. Am. Chem. Soc.* **2006**, *128*, 5650. (e) Puigmartí-Luis, J.; Minoia, A.; Uji-i, H.; Rovira, C.; Cornil, J.; De Feyter, S.; Lazzaroni, R.; Amabilino, D. B. *J. Am. Chem. Soc.* **2006**, *128*, 12602. (f) Florio, G. M.; Klare, J. E.; Psamba, M. O.; Werblowsky, T. L.; Hyers, M.; Berne, B. J.; Hybertsen, M. S.; Nuckolls, C.; Flynn, G. W. *Langmuir* **2006**, *22*, 10003. (g) Nath, K. G.; Ivasenko, O.; Miwa, J. A.; Dang, H.; Wuest, J. D.; Nanci, A.; Perepichka, D. P.; Rosei, F. *J. Am. Chem. Soc.* **2006**, *128*, 4212. (h) Tao, F.; Bernasek, S. L. *Langmuir* **2007**, *23*, 3513.

(8) (a) Xu, B.; Tao, C.; Cullen, W. G.; Reutt-Robey, J. E.; Williams, E. D. *Nano Lett.* **2005**, *5*, 2207. (b) Dmitriev, A.; Spillmann, H.; Stepanow, S.; Strunskus, T.; Woll, C.; Seitsonen, A. P.; Lingenfelder, M.; Lin, N.; Barth, J. V.; Kern, K. *ChemPhysChem* **2006**, *7*, 2197. (c) Schock, M.; Otero, R.; Stojkovic, S.; Hummelink, F.; Gourdon, A.; Laegsgaard, E.; Stensgaard, I.; Joachim, C.; Besenbacher, F. *J. Phys. Chem. B* **2006**, *110*, 12835–12838. (d) Katano, S.; Kim, Y.; Matsubara, H.; Kitagawa, T.; Kawai, M. *J. Am. Chem. Soc.* **2007**, *129*, 2511. (e) Huang, T.; Hu, Z.; Zhao, A.; Wang, H.; Wang, B.; Yang, J.; Hou, J. G. *J. Am. Chem. Soc.* **2007**, *129*, 3857.

(9) Pérez-García, L.; Amabilino, D. B. *Chem. Soc. Rev.* **2007**, *36*, 941.

10.1021/la8017419 CCC: $40.75
Published on Web 07/24/2008

symmetry operation, surface confined patterns formed by these enantiomers also relate to each other by mirror symmetry. Despite many advances in this area, there remain a number of important aspects that lay unexplored. In particular, the way by which a given chiral center leads to enantioselective monolayer formation via molecule−molecule and molecule−substrate interactions is unclear. Here, we focus on a functionalized tetraphenyl porphyrin incorporating four identical stereogenic centers, giving it potential C_4 symmetry, adsorbed onto the C_3 surface of highly oriented pyrolytic graphite (HOPG). By means of scanning tunneling microscopy (STM), we confirm the existence of enantiomorphism: the optical antipodes form mirror-image type molecular patterns. More importantly, molecular modeling and dynamics reveal the precise nature of the chiral induction mechanism in these physisorbed layers.

The adsorption of similar molecules with only long alkyl side groups, but no chiral center or amide group, has already been studied.[10] The authors described the formation of rows of porphyrins separated by a lamella formed by interdigitated alkyl chains. Wang et al.[10b] also showed that one can tune the distance between two rows of porphyrins by changing the length of the alkyl chains, since the alkyl chains are lying flat on the surface. In these studies, the porphyrins are achiral and assemble into achiral arrangements. Here, we apply a multidisciplinary approach (combining the design and the synthesis of the target compound, scanning probe microscopy analysis of the self-assembly, and modeling of the organization within the assemblies) to gain insight into the origin of the expression of chirality in self-assembled monolayers on graphite. More specifically, our main objective is to understand how chirality at the molecular scale can be transferred at the nanoscale.

Results and Discussion

Synthesis. The molecule we targeted for the study (**1**) was selected because it has a rigid C_4 core, which has an element of twist chirality between the porphyrin core and the four phenyl rings appended to it, and has four identical stereogenic centers, four hydrogen bond donor−acceptor groups (the amide moieties), and long alkyl chains to favor adsorption to the graphite. The preparation of this molecule was achieved by condensation of (*R*)-methyl 2-(4-formylphenoxy)propanoate[11] with pyrrole using the Adler methodology[12] (see Experimental Section for details). After purification, the resulting chiral tetra-ester was amidated with *n*-octadecylamine to afford the desired compound, which was purified thoroughly by column chromatography and was fully characterized.

STM Measurements. The self-assembly of **1** on graphite was investigated at the HOPG−liquid interface using STM. The molecules were dissolved in 1-heptanol (saturated solution), and a drop of this solution was applied on the basal plane of HOPG. STM in constant height mode was used to follow the monolayer formation. After a while, the spontaneous formation of highly ordered adlayers of **1** was observed at the 1-heptanol−graphite interface. As the contrast in the STM images reflects differences in tunneling current, bright and dark features correspond to a high and low tunneling current, respectively.

Figure 1A shows a typical STM image of **1** physisorbed at the 1-heptanol−graphite interface. The image is composed of a regular pattern of rows of large bright areas (a little over 1 nm^2),

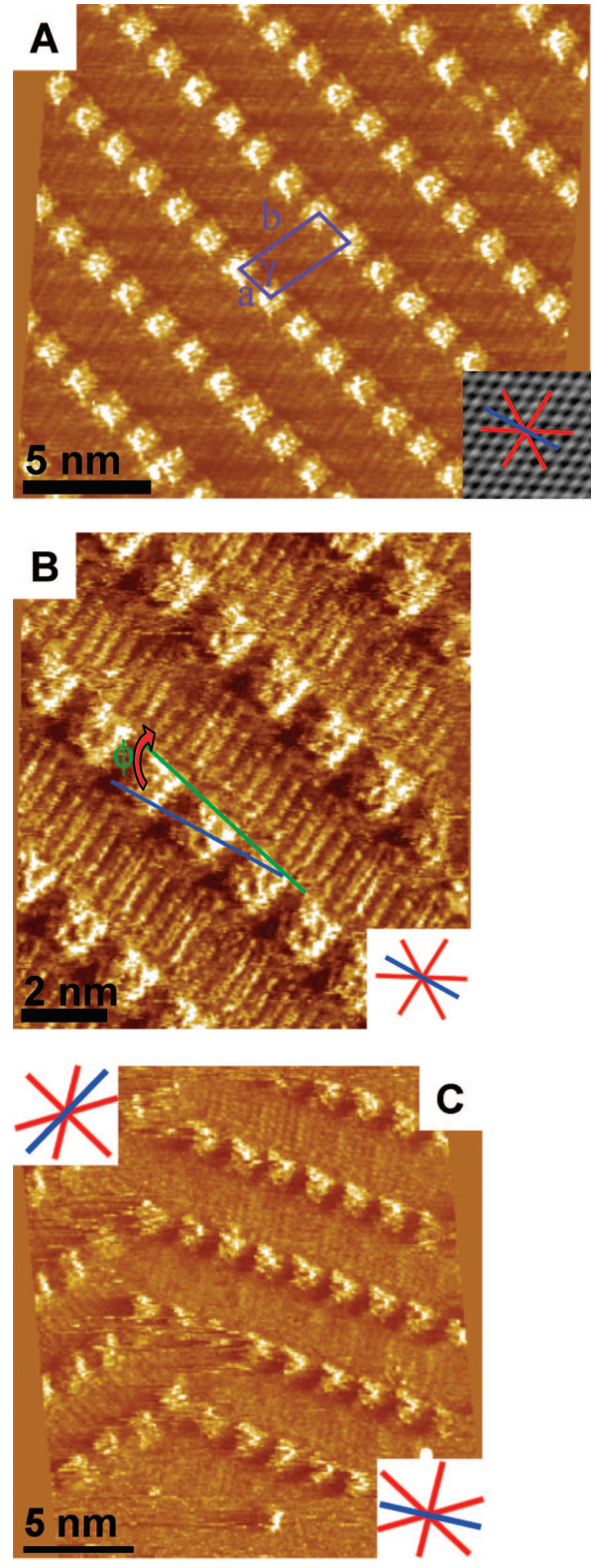

Figure 1. STM images of **1** physisorbed at the interface between graphite and 1-heptanol. The red lines in the insets indicate the direction of the major symmetry axes of graphite (see text). The blue line, running perpendicular to one of the main symmetry axes, is a reference axis selected to evaluate the orientation of the monolayer with respect to the substrate. (A) The unit cell is indicated in purple. The inset shows an STM image of graphite (not to scale). $I_{set} = 0.6$ nA; $V_{set} = -0.396$ V. (B) The blue line is the selected reference axis. The green solid line is the propagation axis of the porphyrin rows. Φ is the angle between the reference axis and the propagation axis. $I_{set} = 0.8$ nA; $V_{set} = -0.428$ V. (C) Image of a domain boundary. Each inset relates to the domain underneath. $I_{set} = 0.8$ nA; $V_{set} = -0.404$ V.

(10) (a) Qui, X.; Wang, C.; Zeng, Q.; Xu, B.; Yin, S.; Bai, C. *J. Am. Chem. Soc.* **2000**, *122*, 5550. (b) Wang, H.; Wang, C.; Zeng, Q.; Xu, S.; Yin, S.; Xu, B.; Bai, C. *Surf. Interface Anal.* **2001**, *32*, 266.

(11) Minguet, M.; Amabilino, D. B.; Vidal-Gancedo, J.; Wurst, K.; Veciana, J. *J. Mater. Chem.* **2002**, *12*, 570.

(12) Adler, A. D. *J. Org. Chem.* **1967**, *32*, 476.

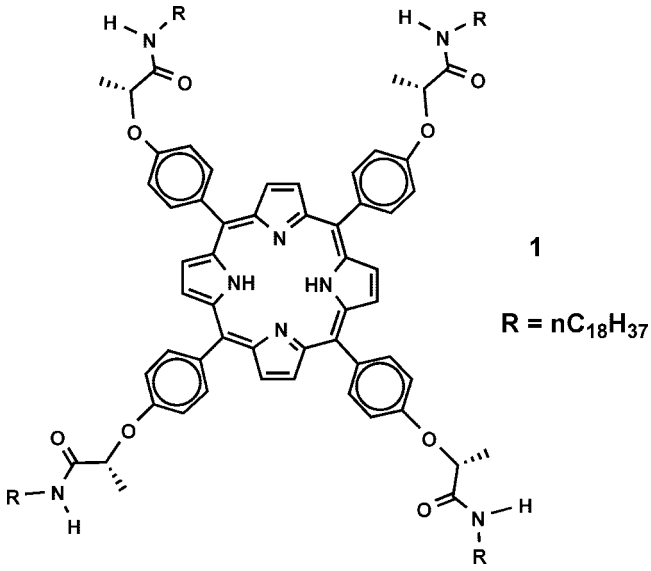

attributed to the porphyrin cores, separated from each other by darker rows containing lines running almost perpendicular to the porphyrin spots. These lines bridging rows of porphyrin groups are attributed to the alkyl chains.

From Figure 1B, which reflects the monolayer structure over a smaller area, we can propose that all alkyl chains are adsorbed on the surface in a fully extended conformation and those of adjacent porphyrin rows are interdigitated. Although the resolution of the images is good, the amide groups and the chiral centers cannot be distinguished. The distance between two porphyrin units, which corresponds to unit cell vector *a,* amounts to 1.9 ± 0.1 nm. The other unit cell parameters are $b = 4.0 \pm 0.1$ nm and $\gamma = 80 \pm 2°$. Using molecular modeling, we determine (with the Tinker package and the MM3 force field; see details in the Computational Methodology section) that the length of the fully extended tail (from the oxygen atom attached to the phenyl ring to the last carbon atom of the tail) is 2.57 nm and the diameter of a tetraphenylporphyrin (i.e., the distance between the carbon atoms at the extremes of opposite phenyl rings) is about 1.46 nm. Thus, the total estimated length of the porphyrin molecule core and one tail, oriented with both tails and the porphyrin ring parallel to the surface, is 4.03 nm. This value is in good agreement with the cell parameter obtained from STM images ($b = 4.0$ nm), which confirms the flat orientation of the tetraphenylporphyrin derivative **1** at the 1-heptanol−HOPG interface.

Figure 1C shows a boundary between two domains that are rotated by roughly 120° with respect to each other. The value of that angle indicates that the self-assembly process is strongly influenced by the HOPG substrate. This interaction can be evaluated in more detail by explicitly comparing the orientation of the monolayer relative to the graphite substrate underneath. The insets in Figure 1 illustrate the orientation of the substrate: the red lines indicate the main symmetry axes of graphite, that is, the equivalent ⟨1 −2 1 0⟩ directions. These directions are identical by virtue of the symmetry of the substrate. (See the Supporting Information for the use of Weber indices to assign directions in HOPG.) The inset in Figure 1A also shows explicitly the graphite substrate (not to scale with the STM image of the monolayer). The alkyl chains run parallel to one of the main symmetry axes of graphite. This phenomenon is frequently observed for alkylated compounds and is attributed to the good match between the distance between methylene groups along the alkyl chain and the graphite crystal lattice along that direction. As the amide groups and chiral centers are not visualized, no direct information is available on their orientation and interaction with adjacent molecules or the substrate. Successful monolayer formation of **1** was observed in 1-heptanol only and not in 1-phenyloctane. This suggests that the molecule−substrate interaction alone is not enough to promote monolayer formation but that the solvent also plays an important role:[13] 1-heptanol can indeed compete with the amide groups for hydrogen bonding and, therefore, weaken homodimerization or higher aggregation of the porphyrin molecules. Apparently, 1-phenyloctane cannot play such a role because no images were obtained. It is therefore likely that the monolayer formed is stabilized by specific solvent interactions.

Chirality of the Monolayers. Inspection of the STM images permits the chiral nature of the domains to be recognized by the oblique shape of the unit cell. The chiral arrangement of achiral porphyrin derivatives by the formation of a rectangular unit cell has been observed previously.[14] In these systems, the monolayers that are formed are not chiral globally because of the presence of enantiomeric domains. In the present system, it is actually more informative to evaluate the monolayer chirality by comparing its orientation versus graphite. We have already seen that the alkyl chains run parallel to one of the main symmetry axes of graphite, expressing the intimate relation between monolayer orientation and graphite symmetry. In the same way, we can evaluate the orientation of a porphyrin row with respect to graphite. Therefore, for each domain, a reference axis was selected, running perpendicular to one of the major symmetry axes of graphite, in order to evaluate the orientation of the monolayer with respect to the substrate. The reference axis selected is the one which forms the smallest angle with the porphyrin rows. The relevant reference axis is indicated in each of the insets as a blue line. In Figure 1B, the reference axis is indicated in the STM image, together with the propagation axis of the porphyrin rows (in green). The porphyrin rows do not run parallel to the reference axis but show an angle of approximately +13° with respect to that direction. In fact, the same orientation is observed in all domains probed: the porphyrin rows are always rotated clockwise with respect to the reference axis by about $+13 \pm 2°$. No exceptions were observed. This result indicates clearly that the stereogenic centers influence strongly the molecule−surface interaction. For an achiral molecule or a chiral molecule where the stereogenic center would not influence the molecule−surface interaction, both positive and negative domains would have been observed. Therefore, as far as the expression of molecular chirality is concerned, this system corroborates the results obtained for other alkylated chiral compounds. The key question now is how the chiral information at the molecular level is transferred to the monolayer level.

Modeling of the Supramolecular Organization. The adsorption and organization of molecules at the solid−liquid interface results from a complex interplay between several noncovalent interactions. The two main driving forces for the adsorption of the porphyrin derivative **1** on graphite are as follows: (i) the $\pi-\pi$ stacking between the π-system of the porphyrin core and the π-orbitals of graphite and (ii) the CH$-\pi$ interactions[15] between the long alkyl tails of the porphyrin and the π-orbitals

(13) (a) Lee, S. Y.; Noh, J.; Hara, M.; Lee, H. *Mol. Cryst. Liq. Cryst.* **2002**, *377*, 177. (b) Mamdouh, W.; Uji-i, H.; Ladislaw, J. S.; Dulcey, A. E.; Percec, V.; De Schryver, F. C.; De Feyter, S. *J. Am. Chem. Soc.* **2006**, *128*, 317. (c) Tao, F.; Goswami, J.; Bernasek, S. L. *J. Phys. Chem. B* **2006**, *110*, 19562.

(14) (a) Qiu, X.; Wang, C.; Zeng, Q.; Xu, B.; Yin, S.; Wang, H.; Xu, S.; Bai, C. *J. Am. Chem. Soc.* **2000**, *122*, 5550. (b) Zhou, Y.; Wang, B.; Zhu, M.; Hou, J. G. *Chem. Phys. Lett.* **2005**, *403*, 140. (c) Otsuki, J.; Nagamine, E.; Kondo, T.; Iwasaki, K.; Asakawa, M.; Miyake, K. *J. Am. Chem. Soc.* **2005**, *127*, 10400.

(15) (a) Nishio, M.; Hirota, M.; Umezawa, Y. *The CH/π interaction: Evidence, Nature and Consequences*; Wiley-VCH: New York, 1998. Each CH$-\pi$ interaction is about 1.0 kcal/mol. (b) Shibasaki, K.; Fujii, A.; Mikami, N.; Tsuzuki, S. *J. Phys. Chem. A.* **2006**, *110*, 4397.

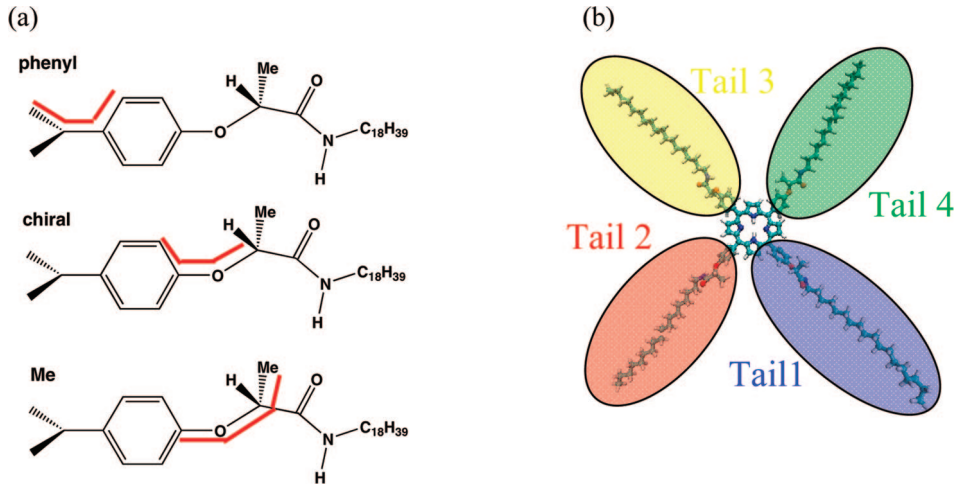

Figure 2. (a) Characteristic dihedral angles defining the conformation of **1**. (b) Labeling of the four tails of **1**.

of graphite. CH$-\pi$ interactions are weak hydrogen bonds occurring between soft acids and soft bases; they are due largely to dispersion and partly to charge-transfer and electrostatic forces. They depend on the orientation of the C−H bond and are additive in enthalpy. In contrast to classical hydrogen bonds, a reduction of the C−H bond length[16] occurs in the presence of CH$-\pi$ interactions. In addition to these interactions, the presence of the amide groups could in principle promote the formation of hydrogen bonds, either among neighbor porphyrin derivatives on the surface or between these molecules and the overlaying solvent.

Before addressing the self-assembly *per se*, it is useful to first investigate the conformational degrees of freedom of **1**, as this information will subsequently be useful to understand the formation of monolayers on graphite. We have thus performed a comparative analysis of the porphyrin geometric structure in vacuum and on the graphite surface.

Besides a slight distortion of the porphyrin core, the four tails of the molecule undergo significant structural rearrangements when deposited onto the graphite surface. These can be probed along molecular dynamics (MD) simulations, through the evolution in time of (i) the dihedral angle between the core of the porphyrin and the phenyl ring (phenyl in Figure 2a); (ii) the dihedral angle defining the position of the stereogenic center (chiral in Figure 2a); and (iii) the dihedral angle associated with the methyl group attached to the chiral center (Me in Figure 2a). The distributions recorded for these three dihedral angles are displayed for the four tails in Figure 3, for the molecule both in vacuum and when adsorbed on graphite. After equilibration, we observe that the tails located opposite to each other around the porphyrin core behave similarly; that is, tails 1 and 3 on one hand and tails 2 and 4 on the other hand are characterized by the same distributions of dihedral angles (Figure 3a). As expected, the phenyl rings are strongly tilted (i.e., by about 45°) with respect to the core, as a result of the steric hindrance between the hydrogen atoms in the ortho positions of the benzene moiety and the pyrrolic protons of the core. Moreover, we notice a broadening of the histograms when the porphyrin molecule is in contact with the surface (Figure 3b) while the average angle remains close to the gas-phase value. We conjecture that this broadening is a result of van der Waals interactions between the graphite surface and the phenyl rings.

A major rearrangement occurs upon adsorption for the dihedral angle defining the position of the chiral center (Figure 3c and d). The populations are found around 0° and ±180° in the gas phase, which means that the chiral center can take two different positions, both coplanar with the phenyl ring. The distribution clearly becomes monomodal and centered around 0° when the porphyrin derivative is adsorbed on the surface. Thus, the rotation around the C(phenyl)−O−C* bond is locked when the molecule is adsorbed, freezing the relative positions of the rest of the side chains with respect to the graphite layer, *vide infra*.

The dihedral angle setting the orientation of the methyl group shows a narrow distribution around −90° in vacuum (Figure 3e). On the graphite surface, a second population centered around −160° appears (Figure 3f). It reflects the tendency of the methyl groups to point toward the surface, so that stabilizing CH$-\pi$ interactions are established with the graphite substrate.

To get a deeper insight into the conformation of **1** on graphite, it is also useful to follow the height of the hydrogen and oxygen atoms of the amide group with respect to the graphite surface during the MD simulations (Figure 4). For the sake of comparison, the relative heights of the chiral center and the carbon atom of the methyl group are also displayed. During the whole MD run, we observe the following:

(i) The average height of the porphyrin core with respect to the graphite surface is about 4.1 ± 0.4 Å (not shown here), that is, a distance that is consistent with $\pi-\pi$ interactions.

(ii) The hydrogen atom of the amide group is continuously pointing at the surface while the oxygen atom of the amide group is continuously oriented upward, which indicates that the amide group has a well-defined, stable orientation. Although this simulation is performed on a "dry surface", it is worth stressing that such a conformation with the C═O groups pointing away from the graphite surface is expected to favor hydrogen bond formation with the solvent, *vide infra*.

(iii) The carbon atom of the methyl group born by the chiral center lies *below* the stereogenic carbon atom, which indicates that this methyl group is also pointing at graphite, consistent with the formation of CH$-\pi$ interactions. Note that this type of arrangement arises from the peculiar architecture of the system studied here, namely, the presence of the chiral center close to the porphyrin core. Another conformation, where the methyl group is pointing away from the surface, has been reported in a molecular dynamics study for a chiral mesogen containing a 1-methylheptyloxy chain.[17a] Experimental evidence also led to the conclusion that the methyl group is pointing away from the

(16) Hobza, P.; Spirko, V.; Selze, H. L.; Schlag, W. *J. Phys. Chem. A* **1998**, *102*, 2501.

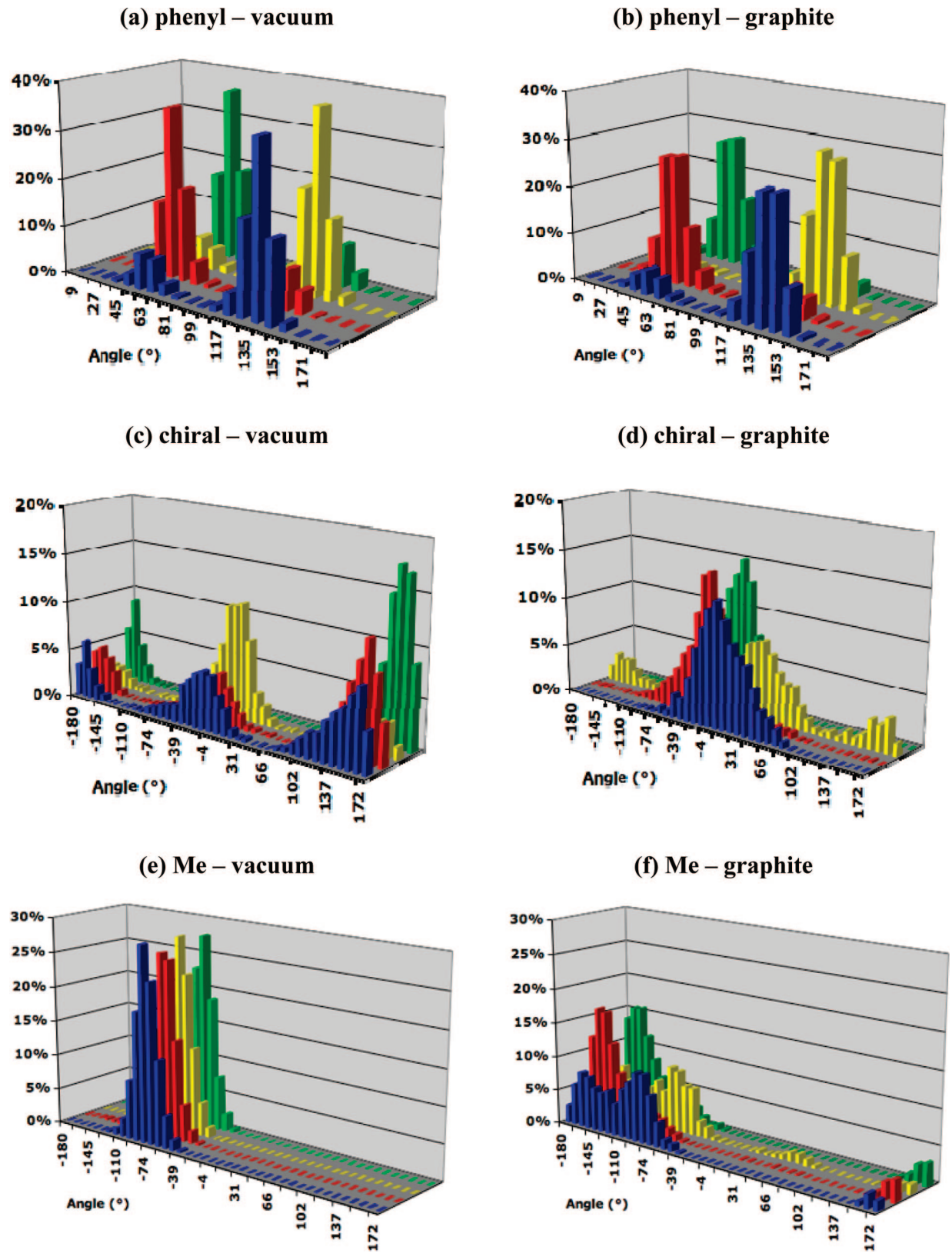

Figure 3. Population of conformers as a function of the phenyl ring dihedral angle in vacuum (a) and on the graphite surface (b); population of conformers as a function of the chiral center dihedral angle in vacuum (c) and on the graphite surface (d); and population of conformers as a function of the methyl dihedral angle in vacuum (e) and on the graphite surface (f). For all the graphics, the color refers to the four tails of the porphyrin (Figure 2b).

surface for self-assemblies of chiral terephthalic acid derivatives where the chiral center on the terminal 2-methylbutoxy group is far away from the aromatic core.[17b] In fact, it might seem counterintuitive to expect that a "bulky" methyl group will point toward the graphite substrate, but the difference between this system and others where the methyl group is pointing away from the surface is the specific location of the chiral center in **1** (next to an amide functionality) and the fact that the phenyl group

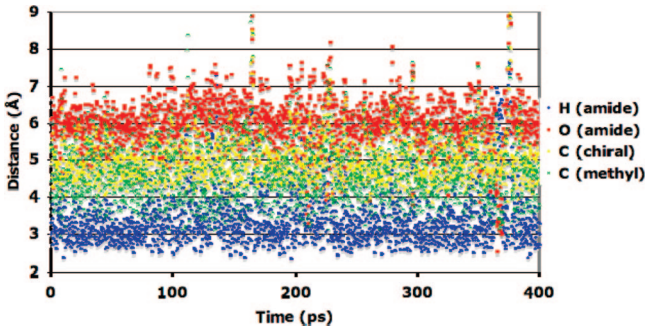

Figure 4. Height (Å) of the hydrogen atom of the amide group (in blue), the oxygen atom of the amide group (in red), the carbon atom of the chiral center (in yellow), and the carbon atom of the methyl group on the chiral center (in green) with respect to the graphite surface during the MD simulation (time in ps). The presence of spikes (at 180 and 380 ps, for example) corresponds to a brief desorption of the tail from the graphite surface.

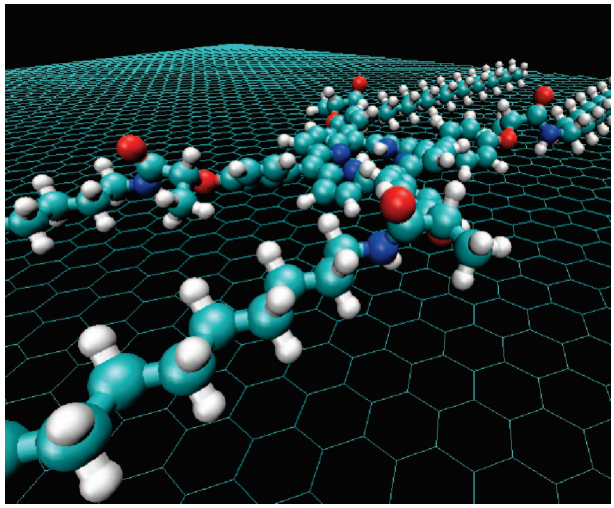

Figure 5. Side view of the optimized structure of **1** adsorbed on graphite. This image illustrates (i) the orientation of the amide groups, with the C═O bonds pointing away from the surface (oxygen atoms in red), and (ii) the orientation of the methyl group toward the surface.

close to the chiral center is tilted, therefore favoring the interaction of the methyl group with the graphite surface. In Figure 5, which shows a side view of the optimized structure of **1** on graphite, one can appreciate the preferential orientation of the methyl group pointing at the surface. This image also illustrates the conformation of the alkyl side chains, which are fully extended and aligned along one direction on the graphite plane.

The structure of the adsorbed porphyrin obtained above was used as a starting point to generate the assemblies. The porphyrin monolayer was built in such a way as to reproduce the density of molecules per unit surface area observed in the STM measurements. Thus, a rectangular 7.2×8.1 nm^2 unit cell of graphite was covered with eight porphyrin molecules, and periodic boundary conditions (PBC) were applied to simulate an infinite adsorbed layer. In order to better understand the relative orientation of the porphyrin rows with respect to the main axes of graphite, the self-assembled structure obtained from the PBC simulations was subsequently extended along the longer axis (b) direction, and laid down at the center of a large graphite slab while revoking the periodic boundary conditions. A MD simulation was run on this structure containing 16 porphyrin molecules. Such a combination of simulations on PBC constrained systems and on larger molecular aggregates is essential for this type of study, in that it ensures that both the density of the self-assembly and its orientation with respect to the substrate surface can be modeled reliably. Upon equilibration, the alkyl chains align perfectly along an axis parallel to one of the main graphite axes (Figure 6a), as is often observed in STM experiments on alkyl chain-containing derivatives. The lattice parameters obtained after equilibration, $a = 1.92 \pm 0.12$ nm, $b = 4.20 \pm 0.14$ nm, $\gamma = 87.4 \pm 4.7°$, are in very good agreement with the STM values (Figure 6a). It is interesting to notice that the formation of such dense monolayers allows for perfect interdigitation between the alkyl chains of molecules in adjacent rows. We also note the presence of a tilt at the end of the alkyl chains close to the porphyrin cores in the next row. The amide groups are not interacting with each other, and the conformation seen in the single molecule modeled on graphite is conserved. This allows for the best space filling and the highest porphyrin density on the graphite surface. Most strikingly, the porphyrin rows (green lines) are tilted with respect to the reference axis of graphite by an angle of $+12.2 \pm 0.4°$. The calculated angle, which is a direct measure of the chiral organization at the surface, is in excellent agreement with the experimental value. We can see from Figure 6b that the methyl groups of the chiral centers of porphyrin **1** (*R,R,R,R*) are pointing to the counterclockwise direction with respect to the porphyrin core (green arrows). As a matter of fact, once a molecule is lying on graphite, its neighbor is expected to shift in a direction perpendicular to the reference axis, so that one of its methyl groups can accommodate in the empty space along the core of the neighboring molecule, between tails 1 and 4 (or 2 and 3). This arrangement allows maximization of the density of the monolayer. The consequence of this shifting is a deviation of the porphyrin-row axis with respect to the reference axis (in blue), which is perpendicular to one of the main graphite axes (in red). A deviation in the opposite direction is expected for the (*S,S,S,S*) enantiomer (Figure 6c).[18] For a mixture of enantiomers, both types of domains (i.e., with $+12°$ and $-12°$ deviation) would probably form, as recently described and explained for 2-bromohexadecanoic acid.[19] The observation of only one type of domain here is the signature of the transfer of chirality from the molecule to the self-assembled layer: the configuration of the chiral center sets the orientation of the methyl group ("clockwise" or "anticlockwise" with respect to the porphyrin core), which in turn sets the deviation of the porphyrin row ($+12°$ or $-12°$) with respect to the substrate reference axis.

As described in the STM section, the self-assembly of **1** has only been observed at the interface between graphite and a protic solvent, 1-heptanol. From the simulations of the adsorbed molecules, we conclude that the amide groups in the porphyrin tails adopt a conformation that is compatible with the formation of hydrogen bonds with overlaying solvent molecules. To confirm this hypothesis, MD simulations were performed on the basis of the equilibrium monolayer while adding one layer of 1-heptanol molecules (Figure 7). We observe that hydrogen bonds with heptanol molecules do form and further stabilize the self-assembled structure, whose inner organization is otherwise not affected by the solvent.

Conclusions

Scanning tunneling microscopy of an enantiomerically pure porphyrin derivative carrying a stereogenic center in each of its

(17) (a) Yoneya, M.; Yokoyama, H. J. *Chem. Phys.* **2001**, *14*, 9532. (b) De Feyter, S.; Gesquière, A.; Grim, P. C. M.; De Schryver, F. C.; Valiyaveettil, S.; Meiners, C.; Sieffert, M.; Müllen, K. *Langmuir* **1999**, *15*, 2817.

(18) We have checked that an assembly of molecules of the (*S,S,S,S*) enantiomer, positioned in the arrangement found here for **1**, is highly unstable, due to strong steric hindrance between the side groups.

(19) Ilan, B.; Berne, B. J.; Flynn, G. W. *J. Phys. Chem. C* **2007**, *111*, 18243.

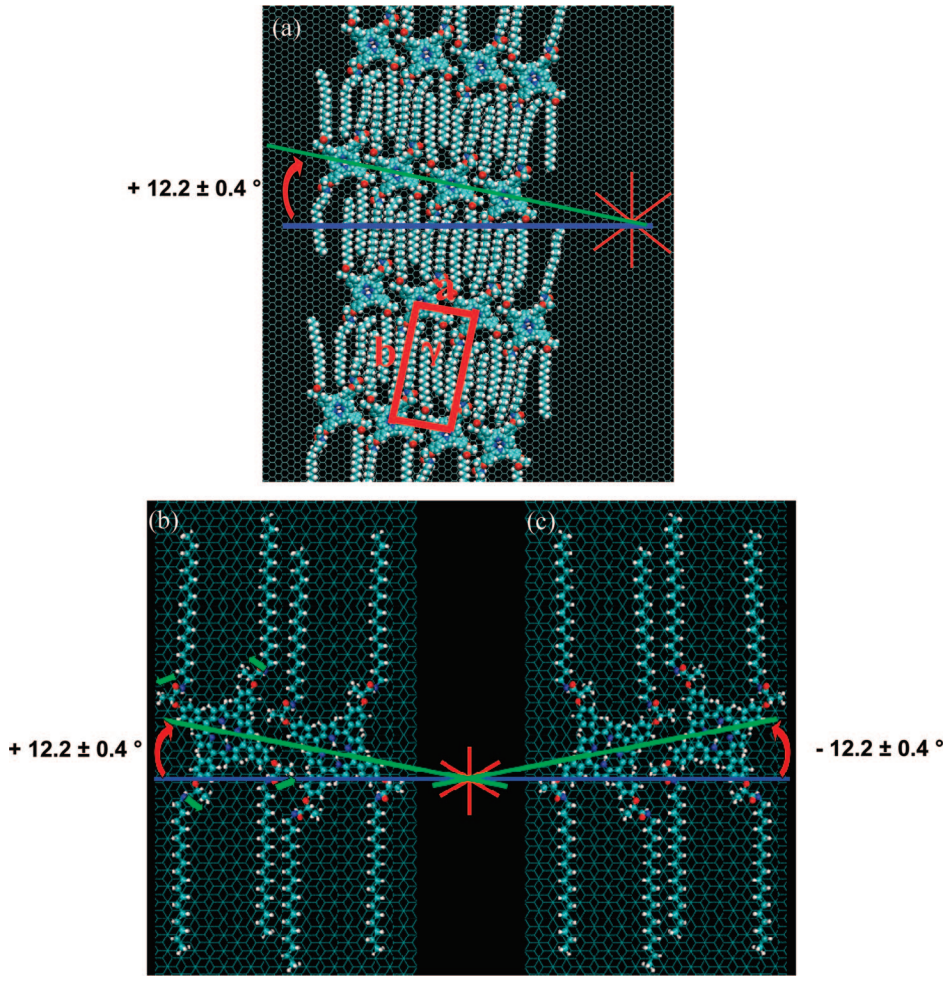

Figure 6. Simulation of the self-assembly of **1** on graphite: (a) Unit cell and illustration of the orientation of the rows of porphyrins with respect to the reference axis of graphite. Top views of (b) the (*R,R,R,R*) porphyrin (**1**) and (c) the corresponding (*S,S,S,S*) enantiomer on the basal plane of graphite. The red lines represent the main axes of graphite. The reference axis (blue line) runs perpendicular to a main symmetry axis of graphite. The green line shows the orientation of a porphyrin row with respect to the reference axis.

four alkylated side chains shows enantiomorphous monolayer formation at the interface between 1-heptanol and graphite. The expression of molecular chirality is most easily identified in the relation of the monolayer orientation with respect to the symmetry elements of the substrate underneath, indicating the importance of molecule−substrate interactions in directing the monolayer growth. These molecules self-assemble on graphite to form an ordered layer with interdigitated alkyl chains that align along one of the graphite axes. The STM experiments confirm the general trend that physisorption of optical antipodes leads to the formation of enantiomorphous monolayers. Force-field molecular dynamics simulations bring insight in the induction mechanism of chirality at surfaces, all the way from a single molecule to the monolayer level. This is made possible by combining the results of simulations on PBC constrained systems and on larger molecular clusters, which is required to reach a quantitative interpretation of layer density and orientation.

Surprisingly and in contrast to other reported systems, the methyl group attached to the stereogenic center is oriented toward the π-system of graphite. Furthermore, to maximize the monolayer density, the porphyrin cores are slightly shifted with respect to one another, which results in an angle between the porphyrin rows and the selected reference axis of graphite. As the alkyl chains run along the main symmetry axes of graphite, the domains must therefore be chiral. This angle provides a direct signature for the chiral expression of the supramolecular arrangement at the surface. Packing constraints in combination with the preferred orientation of the chiral molecules, as far as the orientation of the chiral groups is concerned, determine the experimentally observed and theoretically confirmed enantiomorphism.

Both experiment and theory underline also the importance of the solvent in stabilizing the monolayer structure. Such an organization leaves the amide groups with their C═O heads pointing away from the surface, thereby allowing for formation of hydrogen bonds between the porphyrin derivatives and protic solvent molecules.

Experiment and theory go hand in hand in unraveling the processes involved in the formation of chiral monolayers on surfaces. Studies on the effect of the number of chiral centers and their location on the resulting organization are in progress in our laboratories.

Experimental Section

5,10,15,20-Tetra[4-(*R*,*R*,*R*,*R*)-methyl 2-phenoxy propanoate]-porphyrin. Freshly distilled pyrrole (269 μL, 3.84 mmol) and (*R*)-methyl 2-(4-formylphenoxy)propanoate (800 mg, 3.84 mmol) were added to refluxing propionic acid (14 mL). After refluxing for 90 min, the solution was cooled to room temperature and the propionic acid was removed by careful evaporation in vacuo. The dark viscous material remaining was then washed thrice with hot water to remove remaining propionic acid and other undesired tar. The crude product was subjected to column chromatography (SiO_2, CH_3Cl/MeOH 100:

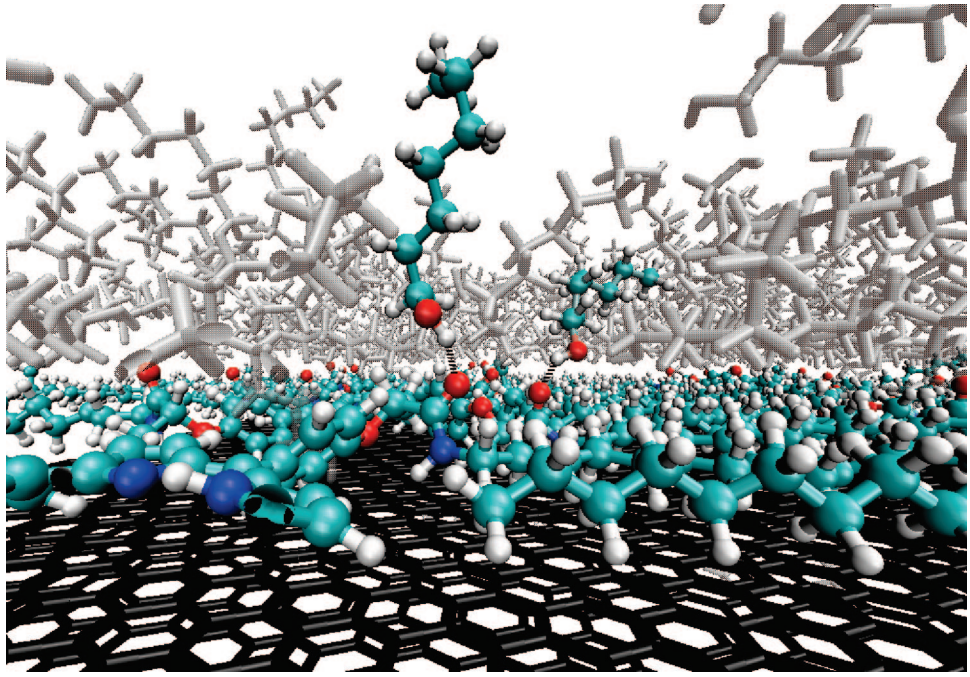

Figure 7. Self-assembly at the interface between graphite and 1-heptanol. The formation of hydrogen bonds with solvent molecules is shown in blue.

0.5) for purification, giving the desired product as a purple solid (700 mg, 18% yield). FT-IR (KBr): 2992 (w, CH_3), 2949 (w, CH_3), 1756 (s, CO), 1736 (s, CO), 1597 (m, phenyl), 1506 (m, phenyl), 1471 (m), 1282 (m), 1204 (s), 1177 (m), 1133 (s, OCH_3), 1098 (m), 806 (m) cm^{-1}. UV−vis ($CHCl_3$) λ_{max}/nm (ε/mol L^{-1} cm^{-1}): 421 (30 613), 518 (1181), 555 (738), 593 (375), 645 (432). ^1H NMR (250 MHz, $CDCl_3$): 8.84 (s, 8H, pyrroleH), 8.10 (d, J = 8.7, 8H, ArH), 7.24 (d, J = 8.5, 8H, ArH), 5.08 (q, J = 6.8, 4H, $ArOCHCH_3COOMe$), 1.83 (d, J = 6.9, 12H, ArH), −2.8 (s, 4H, pyrroleNH) ppm. LDI-TOF/MS m/z (%): 1022.84 (100) $[M]^+$. Elemental anal. (%) calcd: C, 70.44; H, 5.32; N, 5.48. Found: C, 70.56; H, 5.25; N, 5.61.

5,10,15,20-Tetra[4-(*R*,*R*,*R*,*R*)-2-*N*-octadecylamidoethyloxiphenyl]porphyrin (1). 5,10,15,20-Tetra[4-(*R,R,R,R*)-methyl 2-phenoxy propanoate]porphyrin (100 mg, 98 mmol) was mixed with an excess of octadecylamine, and the mixture was heated to 80 °C. The mixture was allowed to react for about 16 h until no trace of starting porphyrin was left (control was done running TLC). The mixture was cooled to give a dark red residue. The product was isolated as a purple solid (156 mg, 81%) after purification by column chromatography (CH_2Cl_2/MeOH 100:1). FT-IR (KBr): 3286 (w, NH), 2924 (s, CH_2), 2852 (s, CH_2), 1657 (s, CO), 1606 (m, phenyl), 1497 (m, phenyl), 1466 (s), 1277 (w), 1235 (m), 1176 (m), 1085 (w), 800 (m) cm^{-1}. UV−vis ($CHCl_3$) λ_{max}/nm (ε/mol L^{-1} cm^{-1}): 421 (45 565), 518 (1391), 554 (887), 593 (320), 649 (344). ^1H NMR (250 MHz, $CDCl_3$): 8.84 (s, 8H, pyrroleCH), 8.14 (d, J = 8.55, 8H, ArH), 7.30 (d, J = 8.6, 8H, ArH), 6.70 (t, J = 5.9, 4H, CONH), 5.02 (q, J = 6.7, 4H, $-O\underline{CH}CH_3CONH-$), 3.48−3.39 (m, 8H, $-CONH\underline{CH_2}$, 1.80 (d, J = 6.9, 12H, $-OCH\underline{CH_3}CONH-$), 1.63−1.59 (m, 8H, $-CONHCH_2-\underline{CH_2}(CH_2)_{15}CH_3$), 1.36−1.16 (m, 120H, $-CONHCH_2CH_2(\underline{CH_2})_{15}-CH_3$), 0.86 (t, J = 6.4, 12H, $-CONHCH_2CH_2(CH_2)_{15}\underline{CH_3}$), −2.8 (s, 2H, pyrroleNH) ppm. LDI-TOF/MS m/z (%): 1971.35 (100) $[M]^+$. Elemental anal. (%) calcd: C, 77.92; H, 9.91; N, 5.68. Found: C, 78.05; H, 9.83; N, 5.77.

General Methods for Materials Characterization. IR spectra were recorded on samples dispersed in KBr pellets in a Fourier transform Perkin-Elmer, Spectrum One spectrometer. ^1H NMR spectra were recorded with a Bruker Avance 250 instrument. Tetramethylsilane or residual solvent protons were used as the internal standard. Laser desorption ionization time-of-flight (LDI-TOF) spectra were recorded on a Maldi2 K-probe (KRATOS ANALYTICAL) mass spectrometer. The spectra were recorded using pulsed extraction of positive ions. The samples were deposited onto the stainless sample plates from chloroform solutions. UV−vis measurements were performed using a Cary 5 UV−vis-NIR instrument from Varian. Flash column chromatography was carried out on silica (35−70 μm) from SDS. The solvents used were distilled using standard methods. Elemental analyses were performed by the London Metropolitan University, STSU, London.

Scanning Tunneling Microscopy. The STM images presented here were obtained at the liquid−solid interface using a Discoverer scanning tunneling microscope (Topometrix Inc., Santa Barbara, CA) along with an external pulse/function generator (model HP 8111 A). STM tips were electrochemically etched from Pt/Ir wire (80%/20%, diameter 0.2 mm) in 2 N KOH/6 N NaCN solution in water. Highly oriented pyrolytic graphite (HOPG, grade ZYB, Advanced Ceramics Inc., Cleveland, OH) was used as a substrate. An almost saturated solution of the compound in 1-heptanol (purchased from Aldrich and used without further purification) was prepared. The fresh solution was applied to the basal plane of freshly cleaved HOPG, and the STM tip was immersed into the solution and scanned. The bias voltage was applied to the sample in such a way that at negative bias voltage electrons tunnel from the sample to the tip. The measured tunneling currents are converted into an image by an A-D converter: a bright (dark) contrast refers to a high (low) current. The setpoint current (I_{set}) and bias voltage (V_{set}) are indicated in the Figure 1 caption. For analysis purposes, the imaging of a molecular layer was immediately followed by recording the graphite lattice at a lower bias voltage, under otherwise identical experimental conditions. Drift effects were corrected by using Scanning Probe Image Processor (SPIP) software (Image Metrology ApS). Note that only images containing a small or no drift were used for analysis.

Computational Methodology. Molecular mechanics and dynamics (MD) simulations were performed with the Tinker package[20] and the MM3 force field,[21] which has been recently reparameterized[22] to take into account the weak nonbonding interactions such as $\pi-\pi$ stacking, CH−π interactions, and hydrogen bonds.

For the conformational analysis, MD simulations were run in the NVT canonical ensemble at 600 K using periodic boundary conditions. For the simulations in vacuum (without graphite), the

(20) http://dasher.wustl.edu/tinker/.
(21) Allinger, N. L.; Yuh, Y. H.; Lii, J. H. *J. Am. Chem. Soc.* **1989**, *111*, 8551.
(22) Ma, B. Y.; Lii, J. H.; Allinger, N. L. *J. Comput. Chem.* **2000**, *21*, 813.

molecule is placed in a large cubic box ($12.0 \times 12.0 \times 12.0$ nm^3) to avoid self-interaction between the molecule and its images. For the simulations on the graphite surface, a periodic two-layer sheet of graphite was built with dimensions 11.9×6.6 nm^2 in the plane of graphite and 5.0 nm in the direction perpendicular to the graphite surface. The graphite structure was frozen during the simulation. In all cases (in vacuum and on graphite), a cutoff of 2.0 nm was applied for the van der Waals interactions. An MD simulation of 400 ps was first performed to equilibrate the system, which was then probed during the subsequent 400 ps (with frames recorded every 0.2 ps).

To study the self-assembly, we used the NVT canonical ensemble at 300 K. Eight porphyrin molecules were adsorbed on the graphite bilayer in a box of 7.2×8.1 nm^2 in the plane of graphite and 5.0 nm in the perpendicular direction to the plane of graphite. A time of equilibration of 200 ps was used, and the lattice parameters were recorded during 200 ps (with steps of 0.2 ps).

In the case of the self-assembly without periodic boundary conditions, we performed MD simulations in the NVT canonical ensemble at 300 K and 16 molecules were laid down on the graphite surface (with size 16.9×24.3 nm^2). The system was first equilibrated by running a 100 ps MD simulation, and the deviation of the porphyrin rows with respect to the graphite reference axis was then investigated in a 100 ps long MD run (with steps of 0.1 ps).

The same periodic box as that used for the self-assembly with PBC was adopted for studying the effect of the solvent. A total of 240 1-heptanol molecules were deposited on top of the porphyrin self-assembled layer.

Acknowledgment. This work was supported by the Dirección General de Investigación, Ciencia y Tecnología (MEC, Spain), under the project CTQ2006-06333/BQU, the DGR, Catalonia (Project 2005 SGR-00591), by the European Union Marie Curie Research Training Network CHEXTAN (MRTN-CT-2004-512161), by the Interuniversity Attraction Pole program of the Belgian Federal Science Policy Office (PAI 6/27), and by FNRS-FRFC.

Supporting Information Available: Representation of the graphite basal plane with the Weber indices; description of the deformation of the porphyrin core when deposited onto the surface; snapshot and lattice parameters of the self-assembly using periodic boundary conditions. This material is available free of charge via the Internet at http://pubs.acs.org.

LA8017419